AME02

The Second TSME International Conference on Mechanical Engineering
19-21 October, 2011, Krabi

A Comparative Study on 6-DOF Trajectory Simulation of a Short Range Rocket using Aerodynamic Coefficients from Experiments and Missile DATCOM

Pawat Chusilp*, Weerawut Charubhun, and Navapan Nutkumhang

Defence Technology Institute (Public Organization)
47/433 Chang Wattana Road, Pakkred, Nonthaburi, Thailand 11120
*Corresponding Author: pawat.c@dti.or.th, Tel: 66 2 980 6612 to 15, Fax: 66 2 980 6688 ext 300

Abstract

A comparative study was carried out to investigate the trajectory simulation of a short range solid propellant rocket using aerodynamic coefficients determined by different methods. The first set of aerodynamic coefficients was estimated using an aerodynamic prediction code, Missile DATCOM. It was found that the accuracy of the predicted coefficients was limited due to the limitation of Missile DATCOM and model simplification. The second coefficient set was obtained from published experimental data and employed as a benchmark. Then these two sets of coefficients were applied to a 6-DOF rigid body model for trajectory simulation. The result parameters, such as spin rate, angle of attack, and impact point, were compared. The comparison suggested that the less accurate coefficients predicted by Missile DATCOM could be used for predicting velocity and impact point of the selected rocket with moderate errors. However, significant error was found in the spin rate and angle of attack prediction.

Keywords*:* Trajectory Simulation, Aerodynamic Coefficients, 6-DOF, Rocket, Missile DATCOM.

List of Symbols

A_{ref}	Reference area, which is equal to rocket cross section area (m^2)
C_A	Axial force coefficient
C_D	Drag coefficient
C_l	Rolling moment coefficient
C_{lp}	Rolling moment coefficient derivative with roll rate (1/rad)
$C_{m\alpha}$	Pitching moment coefficient derivative with angle of attack (1/rad)
$C_{m\dot{\alpha}}$	Pitching moment coefficient derivative with angle of attack rate (1/rad)
C_{mq}	Pitching moment coefficient derivative with pitch rate (1/rad)
$C_{n\beta}$	Yawing moment coefficient derivative with side slip angle (1/rad)
C_{nr}	Yawing moment coefficient derivative with yaw rate (1/rad)
C_{np}	Yawing moment coefficient derivative with pitch rate (1/rad)
$C_{N\alpha}$	Normal force coefficient derivative with angle of attack (1/rad)
$C_{Y\beta}$	Side force coefficient derivative with side slip angle (1/rad)
F_x, F_y, F_z	Aerodynamic forces (N)

M_x, M_y, M_z Aerodynamic moments (N.m)

F_{prop} Propulsive force (N)

M_{prop} Propulsive moment (N.m)

g Acceleration due to Earth's gravity (m/s^2)

I_{xx}, I_{yy}, I_{zz} Rocket moments of inertia ($kg.m^2$)

L_{ref} Characteristic length, which is equal to rocket caliber (m)

m Rocket mass (kg)

p,q,r Rotation components in the body frame (rad/s)

u,v,w Velocity components in the body frame (m/s)

V Total velocity magnitude (m/s)

X_{cp} Center of pressure location measured from nose (m)

X_{cg} Center of gravity location measured from nose (m)

α Angle of attack (rad)

β Side slip angle (rad)

ρ Atmospheric air density (kg/m^3)

ϕ, θ, ψ Rocket attitudes in Earth frame (rad)

1. Introduction

A six degree of freedom (6-DOF) model enables engineers to investigate rocket dynamics during the preliminary design phase [1]. The aerodynamic forces and moments included in the six degree of freedom model are normally calculated using aerodynamic coefficients. These coefficients can be estimated by many methods, which may be categorized into 3 groups [2]: experimental methods, computational fluid dynamics (CFD) methods, and semi-empirical and analytical methods.

Experimental methods obtain aerodynamic coefficients from wind tunnel, ballistic range, or flight tests. Secondly, the CFD methods simulate flow fields and aerodynamic forces by solving a set of fundamental equations, i.e. Navier-Stokes equations, for fluid domains divided into discrete cells. Some advanced CFD techniques also incorporate Rigid Body Dynamics (RBD) into the simulation [2-6]. Finally, the semi-empirical and analytical methods predict aerodynamic coefficients using analytical formula and empirical database.

Among these groups, the semi-empirical and analytical methods are arguably the quickest way to determine aerodynamic coefficients. This advantage makes them suitable for the preliminary design phase, where the rocket performance needs to be evaluated quickly. Aerodynamics softwares that employ semi-empirical and analytical methods are Missile DATCOM, Aeroprediction, PANEL3D, PRODAS, etc. These softwares have been evaluated for various geometry configurations. Although some literatures showed good agreement with experimental data, it was suggested that these softwares cannot give accurate results for every projectile configuration [7-13]. So caution must be taken when using coefficients from these softwares in trajectory simulation.

This paper investigates the accuracy of 6-DOF trajectory simulation using aerodynamic coefficients that were predicted by Missile DATCOM. The rocket chosen for this study was Hydra70, which is a short range solid propellant rocket. Aerodynamics and flight test data of Hydra70 in a published report [14] was used as a benchmark. These coefficients were applied to a 6-DOF trajectory model to simulate spin rate, angle of attack, and impact points, etc. Results from simulation using experimental coefficients were compared to the same simulation using coefficients from Missile DATCOM.

2. Six Degree of Freedom Model

Similar to most literatures, the six degrees of freedom in this study comprises 3 translational components and 3 rotational components. Following assumptions are made:

1) Rocket structure is rigid.
2) Thrust vector is coincident with the rocket longitudinal axis.
3) Product moments of inertia of the rocket are insignificant.
4) Effects from Coriolis, Magnus, and wind are neglected.

Two Cartesian coordinate systems are employed: the body frame and the Earth frame. In the body frame (XYZ), the origin is attached to the rocket center of gravity but the axes do not roll with the rocket body. All axes are orthogonal to each other. The X axis is coincident with the rocket longitudinal axis and X is positive forward. The Y axis is directed out the starboard of the rocket. The Z axis points downward and normal to the X and Y axis, satisfying the right-hand rule.

In the Earth frame (NED), the origin is attached to the launch site. The N and E axis pointed to the geographic north and east respectively. The D axis pointed downward, following the right-hand rule. The orientation of body frame relative to Earth frame is defined by 3 Euler angles (Ø, θ, ψ). Transformation from the body frame to the Earth frame can be done using a rotation matrix.

The 3 translations and 3 rotations are calculated by Eqs. (1) – (6).

$$\dot{u} = \frac{1}{m}\left(F_{propulsion} + F_{axial}\right) - g\sin\theta + rv - qw \quad (1)$$

$$\dot{v} = \frac{1}{m}F_{side} + g\cos\theta\sin\phi + pw - ru \quad (2)$$

$$\dot{w} = \frac{1}{m}F_{normal} + g\cos\theta\cos\phi + qu - pv \quad (3)$$

$$\dot{p} = \frac{1}{I_{xx}}\left\{M_{propulsion} + M_x + \left(I_{yy} - I_{zz}\right)qr\right\} \quad (4)$$

$$\dot{q} = \frac{1}{I_{yy}}\left\{M_y + \left(I_{zz} - I_{xx}\right)pr\right\} \quad (5)$$

$$\dot{r} = \frac{1}{I_{zz}}\left\{M_z + \left(I_{xx} - I_{yy}\right)pq\right\} \quad (6)$$

The aerodynamic forces and moments are determined by Eqs. (7) – (12). Note that the nomenclatures in the equations below are case sensitive.

$$F_{axial} = \frac{1}{2}\rho V^2 A_{ref}\left(-C_A\right) \quad (7)$$

$$F_{side} = \frac{1}{2}\rho V^2 A_{ref}\left(-C_{Y\beta}\beta\right) \quad (8)$$

$$F_{normal} = \frac{1}{2}\rho V^2 A_{ref}\left(-C_{N\alpha}\alpha\right) \quad (9)$$

$$M_x = \frac{1}{2}\rho V^2 L_{ref}\left(C_l + \frac{C_{lp}pL_{ref}}{2V}\right) \quad (10)$$

$$M_y = \frac{1}{2}\rho V^2 L_{ref}\left(C_{m\alpha}\alpha + \left(C_{m\dot{\alpha}} + C_{mq}\right)\frac{qL_{ref}}{2V}\right) \quad (11)$$

$$M_z = \frac{1}{2}\rho V^2 L_{ref}\left(C_{n\beta}\beta + \left(C_{nr}r + C_{np}p\right)\frac{L_{ref}}{2V}\right) \quad (12)$$

3. Aerodynamic Coefficients

3.1. Hydra70 Rocket

The Hydra70 rocket is a short range unguided solid propellant rocket that is aerodynamically stabilized. Besides air-to-surface applications, Hydra70 is also used for surface-to-surface applications in some trainings and experimental works due to its low cost. The configuration selected for this study is the MK66 Mod1 rocket motor mated to M261 warhead, as shown in Fig. 1. It is important to note that M261 warhead is chosen due to the availability of test data [14]. It does not imply that the Royal Thai Armed Forces employs such a submunition warhead.

The rocket is 70 mm in caliber and 1.7 m long. The rocket motor produces a total impulse of 1500 lb-sec approximately, which enables the maximum speed up to Mach 1.8 and maximum range more than 10 km. Fig. 2 shows the nozzle with unfolding wrap-around fins. All fins are beveled at the leading edge and partially at the trailing edge to produce desirable aerodynamic rolling moment characteristic. It is difficult to model these features by semi-empirical or analytical methods. In addition, the nozzle outlet is fluted to providing torque during the power-on period.

Fig. 1 Hydra70 rocket [15]

Fig. 2 Wrap-around fins of MK66 rocket motor

3.2 Aerodynamic Data from Experiments

This study employs the aerodynamics in the unclassified report published by Dahlke and Batiuk at US Army Missile Command [14] as a benchmark. This literature provides experimental data of C_D, $C_{N\alpha}$, C_{mq} , C_l , C_{lp} , and X_{cp} for Hydra70 MK66/M151 and MK66/M261 configurations. The literature also presents the spin rate, Mach number obtained from a flight test. It was described that C_D for power-off period was obtained almost entirely from the actual flight test and C_D for power-on period was determined by adjusting the base pressure drag. $C_{N\alpha}$,C_{mq} , C_l , and C_{lp} were derived based on wind tunnel test data. All coefficients were presented as a function of Mach number only. In addition, C_A and $C_{m\alpha}$ are not presented in the Dahlke and Batiuk [14]. So they are derived from Eqs. (13) and (14).

$$C_A = \frac{(C_D - C_{N\alpha}\alpha \sin\alpha)}{\cos\alpha} \qquad (13)$$

$$C_{m\alpha} = \frac{C_{N\alpha}(X_{cg} - X_{cp})}{L_{ref}} \qquad (14)$$

Furthermore, by assuming 90° rotational symmetry, we have $C_{Y\beta} = C_{N\alpha}$, $C_{n\beta} = -C_{m\alpha}$, and $C_{nr} = C_{mq}$. Although the Hydra70 is actually 120° rotational symmetry, this approximation should be reasonable for a spinning rocket.

3.3. Aerodynamic Data from Missile DATCOM

Missile DATCOM is a semi-empirical code for preliminary missile aerodynamic design. It can predict aerodynamics coefficients of both finned and non-finned projectiles based on empirical data and analytical formula. The original FORTRAN 77 version of Missile DATCOM was developed by the McDonnell Douglas Corporation [16]. The 1997 version was used in this study.

The curvature of wrap-around fins is neglected and the fins are treated as a planar fin for simplification. The diameter step at the fin hinge is not modeled. The beveled leading edge and partially beveled trailing edge of the fin, as shown in Fig. 2, are also neglected. These simplifications could results in prediction errors but the purpose of this study is to investigate the effects of errors in coefficients on trajectory simulation, not to obtain accurate aerodynamic coefficients from Missile DATCOM.

Appendix A shows the aerodynamic coefficients predicted by Missile DATCOM throughout the range of Mach 0.4 to 2.5 and angle of attack -12º to 12º.

3.4. Prediction Accuracy

The ability of Missile DATCOM in predicting aerodynamics for various rocket configurations has been studied in many research works [7-9,12,13]. Some studies were done at the angle of attack up to 90º and speed ranging from subsonic to supersonic. It was suggested that Missile DATCOM was reasonably accurate for simple missile configurations such as Body alone and Body-Tail with low sweep fin angle. For Body-Wing-Tail configurations, errors of predicted C_A , $C_{N\alpha}$, $C_{m\alpha}$ were less than 4% at angle of attack 0º to 20º and 22% at angle of attack 20º to 45º [7,8]. Both over prediction and under prediction were observed. Furthermore, prediction of dynamic derivative coefficients such as C_{mq}, $C_{m\dot{\alpha}}$, C_{lp}, was less accurate than that of static coefficients. Predicted values of dynamic coefficients might have errors up to 30% [7,8].

Despite the fact that the wrap-around fins of MK66 Mod1 rocket motor are curved, the rocket is simply a Body-Tail configuration. So Missile DATCOM should be capable of predicting such aerodynamic characteristics accurately. However, it was found that there are large errors in the predicted roll moment coefficients because some geometric features that affect aerodynamic characteristics could not be input into Missile DATCOM as discussed previously.

Overall, both power-on and power-off C_A are under predicted in supersonic region but over predicted in subsonic region. Fig. 3 compares C_A predicted by Missile DATCOM to C_A derived by Eq. 13 at zero angle of attack. It could be seen that the error of power-on C_A is higher than the error of power-off C_A in most range of Mach number. Furthermore, the magnitudes of $C_{N\alpha}$, C_{mq}, C_l, and C_{lp} are largely under predicted.

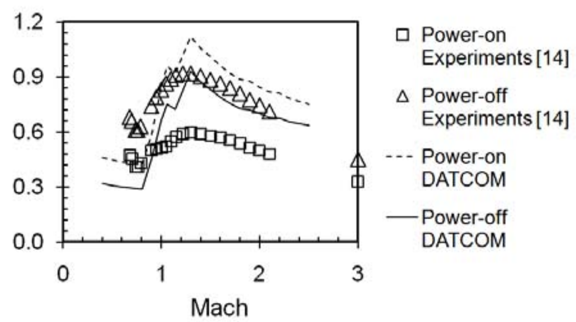

Fig. 3 C_A at zero angle of attack

4. Trajectory Simulation

4.1 Analysis Setup

Four combinations of aerodynamic coefficients, namely EXP, COMBINE1, COMBINE2, and COMBINE3, were applied to the trajectory simulation. EXP consists of aerodynamic coefficients from experiment only. COMBINE1 consists of aerodynamic coefficients from Missile DATCOM but uses C_l and C_{lp} from experimental data. COMBINE2 is similar to COMBINE1 except that it includes only C_{lp}. COMBINE3 consists of all coefficients from Missile DATCOM. Table 1 summarizes the combinations of aerodynamic coefficients used in simulation.

Trajectory simulations were performed at launching elevation angles 30º, 40º, 50º, and 60º for each set of aerodynamic coefficients. Totally, sixteen simulation runs were performed. The fourth order Runge-Kutta method was employed for integration using time step 0.0001 sec.

Table. 1 Aerodynamic coefficient combinations

Coefficient	EXP	COMBINE1	COMBINE2	COMBINE3
C_A	Experiment*	DATCOM	DATCOM	DATCOM
$C_{Y\beta}$	Experiment*	DATCOM	DATCOM	DATCOM
$C_{N\alpha}$	Experiment	DATCOM	DATCOM	DATCOM
C_l	Experiment	Experiment	0**	0**
C_{lp}	Experiment	Experiment	Experiment	DATCOM
$C_{m\alpha}$	Experiment*	DATCOM	DATCOM	DATCOM
C_{mq}	Experiment	DATCOM	DATCOM	DATCOM
$C_{m\dot{\alpha}}$	NA	DATCOM	DATCOM	DATCOM
$C_{n\beta}$	Experiment*	DATCOM	DATCOM	DATCOM
C_{np}	NA	DATCOM	DATCOM	DATCOM
C_{nr}	Experiment*	DATCOM	DATCOM	DATCOM

Experiment = Use experimental data
DATCOM = Obtain from Missile DATCOM
NA = Data not available
* Derived from symmetry or relationship with other coefficients
** The predicted C_l was zero

4.2 Results and Discussion

4.2.1 Range and Drift

The predicted range and drift of impact points from 16 runs are presented in Table 2 and the impact points are illustrated in Fig. 4.

Predicted range from COMBINE1, COMBINE2, COMBINE3 runs are about 18% to 25% greater than EXP runs as shown in Table 2. Moreover, it could be seen that the larger elevation angle, the more error. The over predicted range could be caused by the under predicted predicted C_A in subsonic region hence less drag. Although C_A is over predicted in supersonic region, most of the flight is in subsonic region as shown in Fig. 3.

Table. 2 Range and drift of impact points

Launching Elevation	Coefficients Used	Impact Range			Impact Drift		
		Dist (m)	Error (m)	Error %	Dist (m)	Error (m)	Error %
30 deg	EXP	8,719	-	-	2	-	-
	COMBINE1	10,249	1,530	18%	-12	14	755%
	COMBINE2	10,249	1,530	18%	-10	11	607%
	COMBINE3	10,251	1,532	18%	1	1	33%
40 deg	EXP	9,170	-	-	6	-	-
	COMBINE1	11,129	1,959	21%	-12	19	287%
	COMBINE2	11,129	1,959	21%	-4	11	163%
	COMBINE3	11,130	1,959	21%	10	4	59%
50 deg	EXP	8,913	-	-	12	-	-
	COMBINE1	11,026	2,112	24%	-9	21	168%
	COMBINE2	11,026	2,113	24%	0	13	102%
	COMBINE3	11,025	2,112	24%	23	11	88%
60 deg	EXP	7,883	-	-	19	-	-
	COMBINE1	9,821	1,938	25%	-2	22	113%
	COMBINE2	9,820	1,937	25%	9	10	54%
	COMBINE3	9,820	1,937	25%	41	22	112%

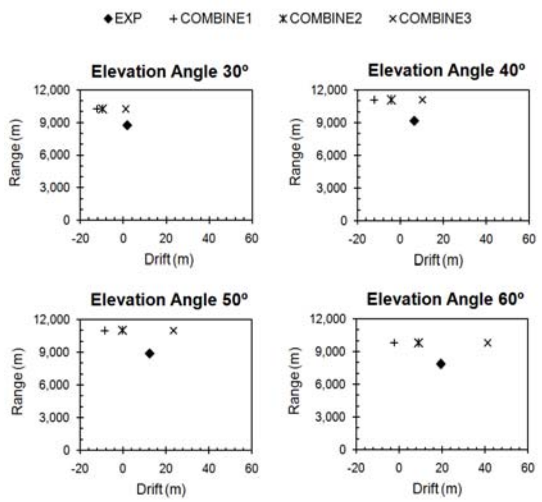

Fig. 4 Predicted impact points

As shown in Table 2, the drift error percentage is more than 700% in some runs. However, the drift error measured in percentage might not be very meaningful. The drift, which is a denominator, is very small so the drift error percentage becomes very large. From the design point of view, small drift error is acceptable because it does not affect rocket sizing and range performance prediction.

Overall, the predicted impact points in COMBINE1 runs are always drifted most leftward and the predicted impact points in COMBINE3 runs are drifted most rightward as shown in Fig. 4. All COMBINE runs uses the same coefficients from Missile DATCOM except C_l and C_{lp}. So the discrepancies could be caused by C_l and C_{lp}.

4.2.2 Spin rate

Fig. 5 compares the spin rate measured from the flight test [14] and all runs at elevation angle 60°. The simulated spin rates at other elevation angles are almost equal so they are not presented here. Note that the elevation angle of the flight is not specified in [14] so this comparison is not conclusive.

It could be seen that EXP, COMBINE1 runs, which applied C_l and C_{lp} from wind tunnel experiments, predicts the spin rate very closed to the flight test data. The COMBINE2 run does not include C_l so there is no induced roll moment and the spin rate ceases quickly after the power-on period. The COMBINE3 run uses C_{lp} from Missile DATCOM, in which the magnitude is much lower than C_{lp} from experiments. Less roll damping force is estimated in COMBINE3 run hence higher predicted spin rate during the power-on period.

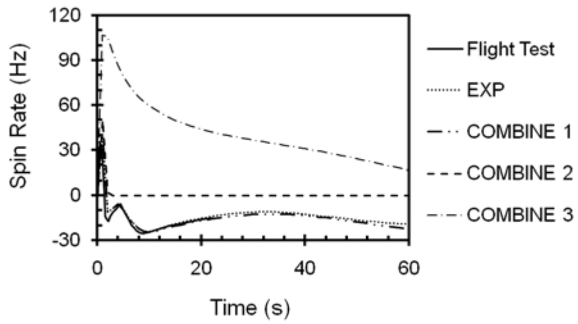

Fig. 5 Spin rate at elevation 60°

4.2.3 Velocity

Fig. 6 compares the Mach number measured from the flight test [14] to COMBINE1 runs. The results from COMBINE2, COMBINE3, and COMBINE4 runs, which also employ C_A from Missile DATCOM, are almost the same as COMBINE1, so they are not presented here. For all curves, the Mach number increases sharply to supersonic at the first 1 sec then decreases to subsonic after the first 8 sec.

It could be seen that the simulated Mach number is close to the flight test data but the predicted maximum Mach number during the first two seconds is lower than the flight test data. However, as previously stated, the comparison is not conclusive due to the fact that the elevation angle of the flight test is not specified.

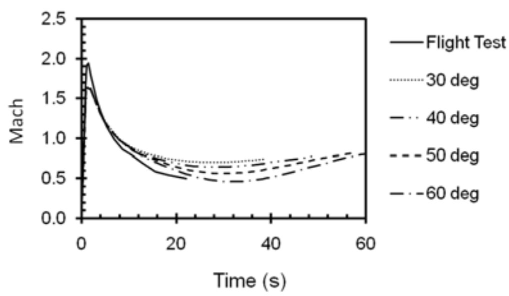

Fig. 6 Mach number from COMBINE1 runs

4.2.4 Angle of attack

Fig. 7 shows the simulated angle of attack and side slip angle of all runs at elevation angle 60º. The data at other launching elevation angles, which is not presented, follows the same trend but smaller in magnitude.

The EXP run predictes much smaller angle of attack and side slip angle than other COMBINE runs. This result was expected because the magnitude of C_{mq} from experiments is much higher than those of $C_{m\alpha}$, $C_{m\dot{\alpha}}$, C_{mq} from Missile DATCOM. So the actual damping force is higher than the simulated ones.

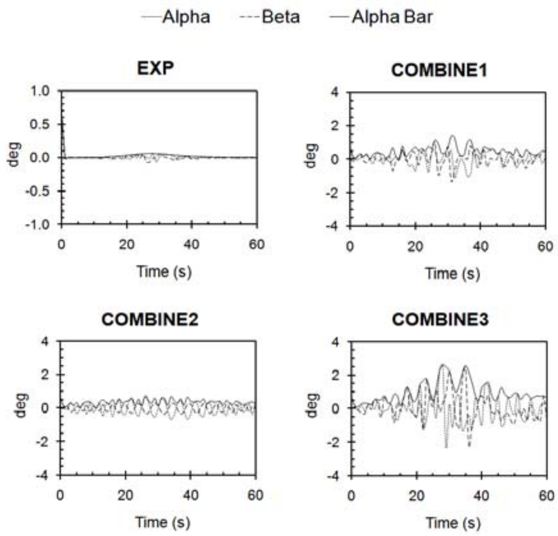

Fig. 7 Angle of attack at elevation 60º

5. Conclusion

In summary, the prediction of impact range using coefficients from Missile DATCOM could give errors up to 25%. Impact drift errors are much smaller than impact range errors if considered in the net distance. The greater launching elevation, the more errors in theh predicted range and drift. The predicted Mach number is close to the flight test data. The simulated angle of attack, side slip angle, and spin rate are inaccurate.

So it could be recommended for the selected rocket that the aerodynamic coefficients predicted by Missile DATCOM are used for impact range and Mach number only.

6. References

[1] Design of Aerodynamically Stabilized Free Rocket (1990). MIL-HDBK-762, US Army Missile Command, AL, USA.

[2] Bartowitz, M. E. (2008). Determination of static and dynamic stability coefficients using Beggar, Master Thesis, Air Force Institute of Technology, Wright-Patterson Air Force Base, OH, USA.

[3] Sahu, J. (2005). Time-accurate numerical prediction of free flight aerodynamics of a finned projectiles, *AIAA Atmospheric Flight Mechanics Conference and Exhibit*, AIAA 2005-3817, San Francisco, CA, USA.

[4] Kokes, J., Costello, M., and Sahu, J. (2006). Generating an aerodynamic model for projectile flight simulation using unsteady time accurate computational fluid dynamic results, ARL-CR-577, Army Research Laboratory, Aberdeen Proving Ground, MD, USA.

[5] Sahu, J. (2007). Unsteady flow computations of a finned body in supersonic flight, ARL-TR-4230, Army Research Laboratory, Aberdeen Proving Ground, MD, USA.

[6] Costello, M., Gatto, S., and Sahu, J. (2007). Using computational fluid dynamics-rigid body dynamic (CFD-RBD) results to generate aerodynamic models for projectile flight simulation, ARL-TR-4270, Army Research

Laboratory, Aberdeen Proving Ground, MD, USA.

[7] Sooy, T. J. and Schmidt, R. Z. (2005). Aerodynamic predictions, comparisons, validations using Missile DATCOM (97) and Aeroprediction 98 (AP98), *Journal of Spacecraft and Rockets*, vol. 42(2), 2005, pp 257-265.

[8] Abney, E. J. and McDaniel, M. A. (2005). High angle of attack aerodynamic predictions using Missile DATCOM, *the 23rd AIAA Applied Aerodynamics Conference*, Toronto, Ontario, Canada.

[9] Sigal, A. (2007). Comparative aerodynamic analysis of a missile with an eight-fin tail, *the 23rd International Symposium on Ballistics*, Tarragona, Spain.

[10] Lesieutre, D. J., Love, J. F., Dillenius, M. F. E., and Blair Jr., A. B. (2002). Recent applications and improvements to the engineering-level aerodynamic prediction software MISL3, *the 40th AIAA Aerospace Sciences Meeting*, Reno, NV, USA.

[11] Atik, H., Erdem, B., Ilgaz, M., Kargancioglu, I. M., Katirci, A., Mahmutyazicioglu, E., and Yalcin, L. (2008). Prediction capabilities and comparison of panel, semi-empiric and CFD codes for missile aerodynamic analysis, *the 26th AIAA Applied Aerodynamics Conference*, Honolulu, HI, USA.

[12] Teo, H. H. (2008). Aerodynamic predictions, comparisons, and validations using Missile Lab and Missile DATCOM (97), Master Thesis, Naval Postgraduate School, CA, USA.

[13] Horton, A. N. and McDaniel, M. A. (2005). Identification and correction of axial force prediction discrepancies due to angle of attack effects in Missile DATCOM, AIAA 2005-4833, *the 23rd AIAA Applied Aerodynamics Conference*, Toronto, Canada.

[14] Dahlke, C. W. and Batiuk, G. (1990). Hydra 70 MK 66 aerodynamics and roll analysis, TR-RD-SS-90-6, US Army Missile Command, Redstone Arsenal, AL, USA.

[15] Field Manual 1-140: Helicopter Gunnery (1996). United States Army, USA.

[16] Missile DATCOM User's Manual (1998). AFRL-VA-WP-TR-1998-3009, US Air Force Research Laboratory, USA.

Appendix A: Aerodynamic Coefficients from Missile DATCOM

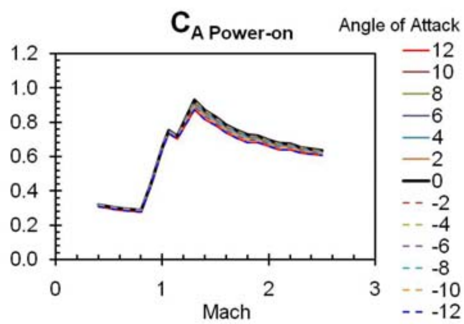

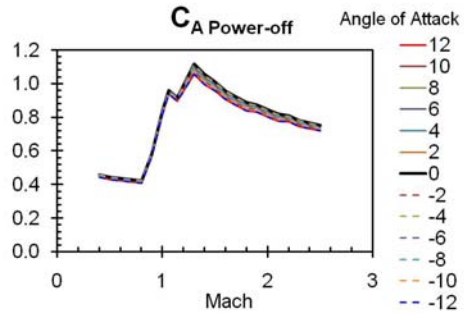

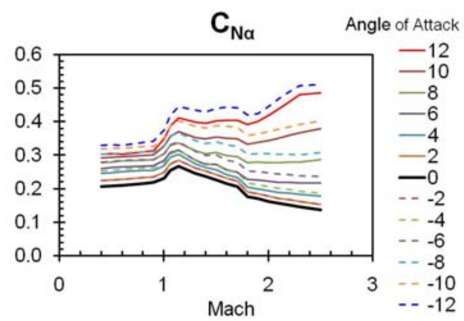

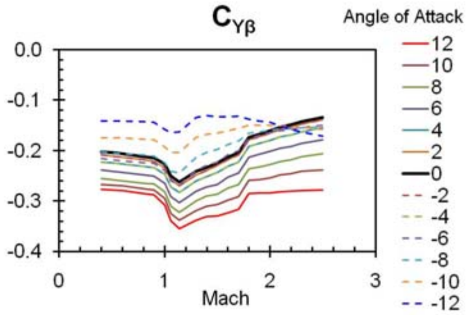
$C_{Y\beta}$
Angle of Attack
12
10
8
6
4
2
0
-2
-4
-6
-8
-10
-12
0.0
-0.1
-0.2
-0.3
-0.4
0
1
2
3
Mach

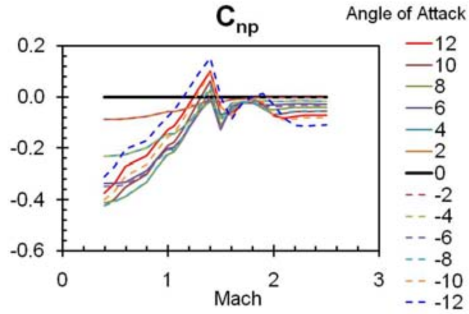
C_{np}
Angle of Attack
12
10
8
6
4
2
0
-2
-4
-6
-8
-10
-12
0.2
0.0
-0.2
-0.4
-0.6
0
1
2
3
Mach

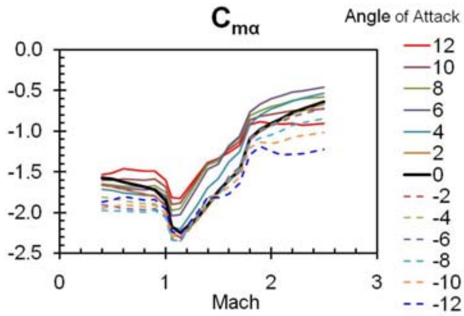
$C_{m\alpha}$
Angle of Attack
12
10
8
6
4
2
0
-2
-4
-6
-8
-10
-12
0.0
-0.5
-1.0
-1.5
-2.0
-2.5
0
1
2
3
Mach

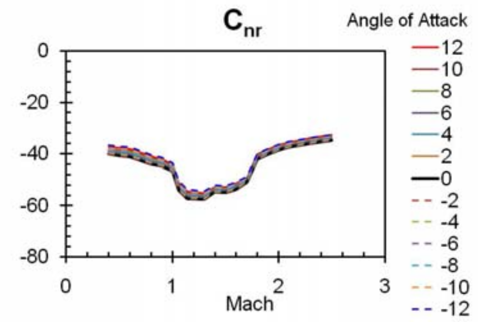
C_{nr}
Angle of Attack
12
10
8
6
4
2
0
-2
-4
-6
-8
-10
-12
0
-20
-40
-60
-80
0
1
2
3
Mach

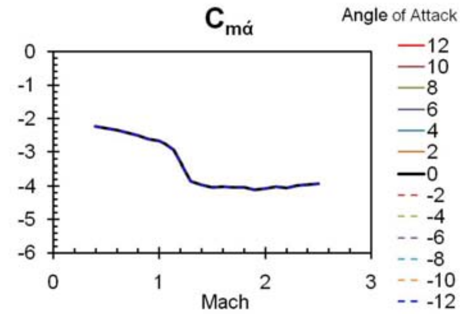
$C_{m\acute{\alpha}}$
Angle of Attack
12
10
8
6
4
2
0
-2
-4
-6
-8
-10
-12
0
-1
-2
-3
-4
-5
-6
0
1
2
3
Mach

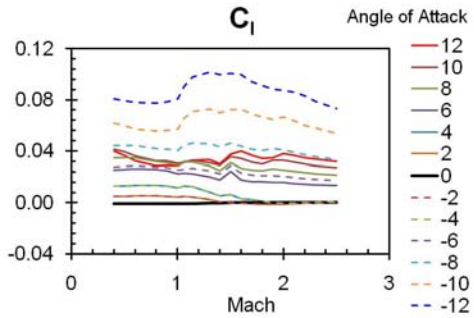
C_l
Angle of Attack
12
10
8
6
4
2
0
-2
-4
-6
-8
-10
-12
0.12
0.08
0.04
0.00
-0.04
0
1
2
3
Mach

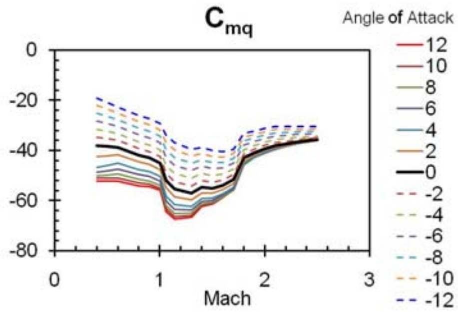
C_{mq}
Angle of Attack
12
10
8
6
4
2
0
-2
-4
-6
-8
-10
-12
0
-20
-40
-60
-80
0
1
2
3
Mach

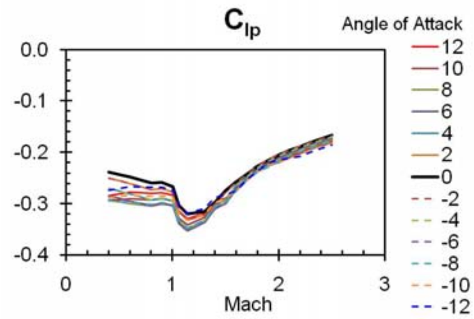
C_{lp}
Angle of Attack
12
10
8
6
4
2
0
-2
-4
-6
-8
-10
-12
0.0
-0.1
-0.2
-0.3
-0.4
0
1
2
3
Mach

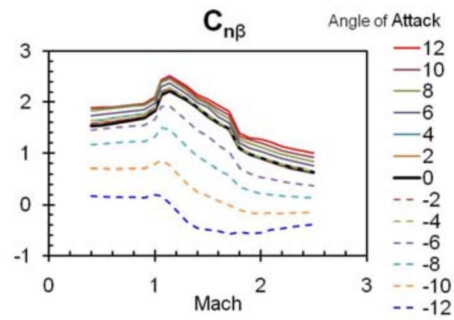
$C_{n\beta}$
Angle of Attack
12
10
8
6
4
2
0
-2
-4
-6
-8
-10
-12
3
2
1
0
-1
0
1
2
3
Mach

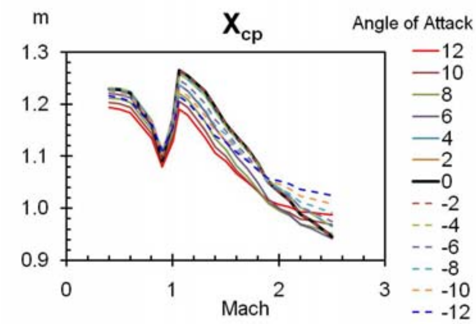
m
X_{cp}
Angle of Attack
12
10
8
6
4
2
0
-2
-4
-6
-8
-10
-12
1.3
1.2
1.1
1.0
0.9
0
1
2
3
Mach